

Capping and Dynamic Relation Between Domains 1 and 2 of Gelsolin

JEANNE FEINBERG, OLIVIER KWIATEK, CATHERINE ASTIER, SEVERINE DIENNET, JEAN MERY, FRÉDÉRIC HEITZ, YVES BENYAMIN and CLAUDE ROUSTAN

Centre de Recherches de Biochimie Macromoléculaire du CNRS, UMR5539, Laboratoire de Recherche sur la Motilité Cellulaire (EPHE), Montpellier Cedex, France

Received 1 April 1997

Accepted 15 May 1997

Abstract: Gelsolin is a protein that severs and caps actin filaments. The two activities are located in the N-terminal half of the gelsolin molecules. Severing and subsequent capping requires the binding of domains 2 and 3 (S2–3) to the side of the filaments to position the N-terminal domain 1 (S1) at the barbed end of actin (actin subdomains 1 and 3). The results provide a structural basis for the gelsolin capping mechanism. The effects of a synthetic peptide derived from the sequence of a binding site located in gelsolin S2 on actin properties have been studied. CD and IR spectra indicate that this peptide presented a secondary structure in solution which would be similar to that expected for the native full length gelsolin molecule. The binding of the synthetic peptide induces conformational changes in actin subdomain 1 and actin oligomerization. An increase in the polymerization rate was observed, which could be attributed to a nucleation kinetics effect. The combined effects of two gelsolin fragments, the synthetic peptide derived from an S2 sequence and the purified segment 1 (S1), were also investigated as a molecule model. The two fragments induced nucleation enhancement and inhibited actin depolymerization, two characteristic properties of capping. In conclusion, for the first time it is reported that the binding of a small synthetic fragment is sufficient to promote efficient capping by S1 at the barbed end of actin filaments. ©1998 European Peptide Society and John Wiley & Sons, Ltd.

Keywords: gelsolin; actin; capping proteins; synthetic peptides

Abbreviations: ELISA, enzyme-linked immunosorbent assay; F-actin, filamentous actin; G-actin, globular actin; 1,5-I-AEDANS, *N*-iodoacetyl-*N*-(5-sulpho-1-naphthyl)ethylenediamine; NbdCl, 7-chloro-4-nitroso-2-oxo-1,3 diazole; TFE, 2,2,2-Trifluoro-ethanol.

Address for correspondence: Claude Roustan, Centre de Recherches de Biochimie Macromoléculaire (CNRS), BP 5051, 34033 Montpellier Cedex, France.

© 1998 European Peptide Society and John Wiley & Sons, Ltd.
CCC 1075-2617/98/020116-12

INTRODUCTION

The cytoskeleton is organized dynamically and can quickly rearrange itself in response to extracellular signals. Actin microfilaments are major components of this network and essential to cell motility, cellular secretion and macromolecular intracellular movements. The formation of stable actin polymers and their rearrangement are thus implicated in many cellular processes. Microfilament remodelling occurs as a result of actin polymerization and depolymerization. Numerous studies have shown the part played by individual proteins in modulating

these transformations. Capping proteins play an important role because of their activity in the vicinity of cellular membranes or Z lines in muscular cells. The study of Nachmias *et al.* [1] illustrates this activity *in vivo*, showing the involvement of capZ during platelet activation: capZ translocation is observed when new barbed ends appear following the uncapping of the existing filaments. Most capping proteins bind actin filaments at the barbed end and enhance the nucleation step during actin polymerization [2]. Proteins of the gelsolin family are unique in being able both to sever and to cap actin filaments [3, 4]. Gelsolin implication *in vivo* is illustrated in experiments conducted by Cunningham *et al.* [5] in which gelsolin overexpression in fibroblasts leads to enhanced cell motility. The studies of Watts [6] on the association of gelsolin with F-actin in polymorphonuclear leucocytes also suggest a role for gelsolin in the formation and regulation of short cytoplasmic filaments.

Gelsolin binds to both monomeric and filamentous actin and is composed of six homologous domains called S1–6 [7]. The N-terminal half of gelsolin is necessary for capping and severing, in particular the S1–2 domains, whereas the C-terminal half is concerned with calcium regulation [8, 9]. Domain 1 interacts with monomeric actin, inhibiting actin polymerization [10], and also binds to the end of actin filaments [11, 12]. Domain 2, in contrast, interacts preferentially with F-actin, its interface being located on the side of the microfilaments [3, 13, 14]. Interaction across the filament axis has also been postulated [15].

According to the model recently described [12, 13, 16], the key steps in severing and capping are: first, the binding of domain 2 to the filament, followed by interaction of domain 1 with two adjacent actin monomers along the filament axis, correlated with dissociation of at least the two actin monomers, leading to severing. The gelsolin that remains bound forms a stable cap at the barbed end of the released filament [13].

We attempt to show how domains 1 and 2 are involved in the process, in order to provide a structural basis for the gelsolin-induced capping mechanism. Since the first kinetic step would include the binding of domain 2 to actin [13, 16], a peptide covering one binding site in this gelsolin domain was synthesized and its structural and functional properties were studied. Furthermore, as domains 1 and 2 appear to act in conjunction one with another in the capping process, the combined effect on actin polymerization of the

synthetic peptide derived from domain 2 and the purified domain 1 was studied as a model. Judging from the nucleation enhancement and the inhibition of actin depolymerization, two characteristic properties of capping proteins, we conclude that this combination can efficiently cap actin filaments in the same way as gelsolin, although with a lower activity.

MATERIAL AND METHODS

Proteins and Peptides

Rabbit skeletal muscle actin was isolated from acetone powder [17]. Actin was labelled at Cys 374 using 1.5-I-AEDANS [18] or pyrenyl iodoacetamide [19]. Bovine plasma gelsolin was purified as described by Soua *et al.* [20]. Domain 1 was obtained by chymotryptic cleavage of gelsolin and purified as previously described [21]. CapZ was purified from fish muscle (unpublished data).

Synthetic peptide derived from sequence 159–174 of gelsolin (peptide 159–174) was prepared from Fmoc-L-Lys (biotin)-Pal-PEG-PS resin with a 9050 Milligen PepSynthesizer (Millipore, UK) according to the Fmoc/tBu system. The crude peptide was deprotected and released by conventional TFA treatment as the C-terminal Lys(biotin)-amide derivative and thoroughly purified by preparative reverse-phase HPLC. The purified peptide was shown to be homogeneous by analytical HPLC: retention time = 10.8 min, on Aquapore RP 300 column, C8, 7 μ m, 220 \times 4.6 mm (Brownlee Lab., Applied Biosystems, San Jose, CA, USA) eluted with a linear gradient of acetonitrile in TFA 0.1%, 0–40% for 15 min (1.5 ml/min). The electrospray mass spectrum, carried out in the positive ion mode using a Trio 2000 VG Biotech Mass spectrometer (Altrincham, UK), was in line with the expected structure (MH^+ at $M/z = 2264.2 \pm 0.9$; theoretical 2265).

Peptide 159–174 was labelled at the amino groups with 7-chloro-4-nitroso-2-oxo-1.3 diazole (NbdCl) [21]. Excess reagent was eliminated by sieving through a Biogel P2 column.

Molecular weight was determined on HPLC using a Bio-Rad TSK 250 column (Bio-Rad Laboratories) equilibrated with 0.1 M Tris buffer, pH 7.5.

Actin solution viscosities were measured with a 0.5 ml Ostwald viscometer (outflow time = 120 s for water) at 20 °C in 2 mM Tris, 0.1 mM ATP, 0.1 mM $CaCl_2$ buffer pH 7.5. Relative viscosities were determined as the ratio of the sample flow time to

that of the reference and specific viscosities as relative viscosity minus 1.

The 159–174 sequence was modelled using the Swiss-model automated protein modelling server. The basic programs used to generate the homologous model need sequence alignments and the known 3D structure of a related protein. In our case, the structure of severin determined by RMN was used [22]. Building of the model was performed using ProMod methods [23] and refined by energy minimization (CHARMm program) [24].

Protein concentrations were determined by UV absorbance [25].

Immunological Techniques

ELISA, previously described in detail [26], was used to monitor interaction between biotinylated peptides and coated actin. Actin in 50 mM NaHCO₃/Na₂CO₃, pH 9.5, was immobilized on plastic microtitre wells. The plastic was then saturated with 0.5% gelatin/3% gelatin hydrolysate in 140 mM NaCl/50 mM Tris buffer, pH 7.5. Binding was monitored at 405 nm using alkaline phosphatase-labelled streptavidin (dilution 1/1000). Control assays were carried out in wells saturated with gelatin and gelatin hydrolysate used alone. Each assay was conducted in triplicate and the mean value plotted after subtraction of non-specific absorption. Additional details on the different experimental conditions are given in the figure legends.

Fluorescence Measurements

Fluorescence experiments were conducted using an LS 50 Perkin-Elmer luminescence spectrometer. Intrinsic fluorescence spectra were obtained for actin in 2 mM Tris, 0.1 mM ATP, 0.1 mM CaCl₂, pH 7.5, at 25 °C. The excitation wavelength was set at 290 nm and the emission spectrum recorded between 310 and 400 nm. Spectra for dansylated actin were obtained in the same conditions, with the excitation wavelength set at 340 nm. Fluorescence changes were deduced from the area of the emission spectra.

Nbd-labelled peptide was incubated in 2 mM Tris buffer, pH 7.5, containing 0.2 mM CaCl₂, 0.1 mM ATP, 2 mM MgCl₂ and 0.1 M KCl at 25 °C and the change in fluorescence polarization monitored after addition of increasing concentrations of F-actin. Excitation and emission wavelengths were set at 476 and 530 nm respectively. The fluorescence polarization of dansylated G-actin in the presence

of synthetic peptide 159–174 was also determined, with the excitation and emission wavelengths set at 340 and 500 nm respectively.

Fourier Transform IR Measurements

Fourier transform IR spectra were recorded using an IFS 28 Bruker spectrometer. Samples were placed in a horizontal ATR plate and the spectra recorded at room temperature. The peptide was analysed at a concentration of 5 mg/ml in 10 mM phosphate buffer, pH 7.5. Five hundred scans were accumulated in the 1800–1500 cm⁻¹ range. The Bruker OPUS/IR 2 program was used for spectrum analysis (second derivative and deconvolution).

Circular Dichroism Measurements

CD spectra were obtained using a Jobin Yvon Mark V dichrograph and 0.1 cm pathlength quartz cells. Data were collected within the 190–260 nm wavelength range. Four scans of each sample were accumulated.

Actin Polymerization

Actin polymerization was monitored by fluorescence. Fluorescence enhancement of pyrenyl-actin was used as an indicator of actin polymerization [27]. Excitation and emission wavelengths for pyrenyl-actin were set at 365 and 386 nm respectively. Polymerization of actin in 2 mM Tris, 0.2 mM CaCl₂, 0.1 mM ATP buffer, pH 7.5, was induced by adding 2 mM MgCl₂ and 0.1 M KCl.

	159	174
sequence	PNEWVQRL	FQVKGRVVRATEVPVS
prH	00000	01000000000000000000
prE	00255668888631247888887730	
prL	99643220001268751111111259	
prediction	LL...EEEEEE	LL.EEEEEEE.L

Figure 1 Secondary structure prediction for peptide 159–174. Prediction was obtained by using the PHD method (see Material and Methods). PrH, prE and prL are the probabilities for assigning helix, strand and loop respectively. The probabilities are on a scale of 0–9. Prediction for all residues with an expected average accuracy > 82%. '.' means that no prediction is made for the residue.

RESULTS

Sequence Involved in the Side Binding of Gelsolin

The N-terminal part of gelsolin domain 2 is directly involved in the actin-gelsolin interface, judging from results obtained previously [12, 28]. One of the phosphoinositide regulation sites on gelsolin is located in subdomain 2. A synthetic peptide based on the sequence of this site, including residues 150–169 [28], interacted not only with inositol phosphates but also with actin. The properties of gelsolin fragments obtained by deletional mutagenesis [12] suggested a more precise location for the actin binding site within sequence 161–173. The latter result prompted us to synthesize the corresponding peptide of sequence 159–174 (Figure 1).

The interaction of the derived synthetic peptide (sequence 159–174) was tested with actin and monitored by ELISA. The binding of the synthetic biotinylated peptide to coated F-actin was revealed with alkaline phosphatase-labelled streptavidin. The results of ELISA experiments presented in Figure 2 show that the peptide interacts with filamentous actin with an apparent K_d of $4 \mu\text{M}$. This was confirmed in solution using fluorescence polarization. The peptide was labelled with NbdCl and incubated in the presence of increasing F-actin concentrations. As shown in the Figure 2 inset, enhanced fluorescence polarization was observed. The saturation curve observed suggests a specific interaction of the peptide with actin. Interaction with a non-related protein (creatine kinase) was also reported as a negative control (Figure 2).

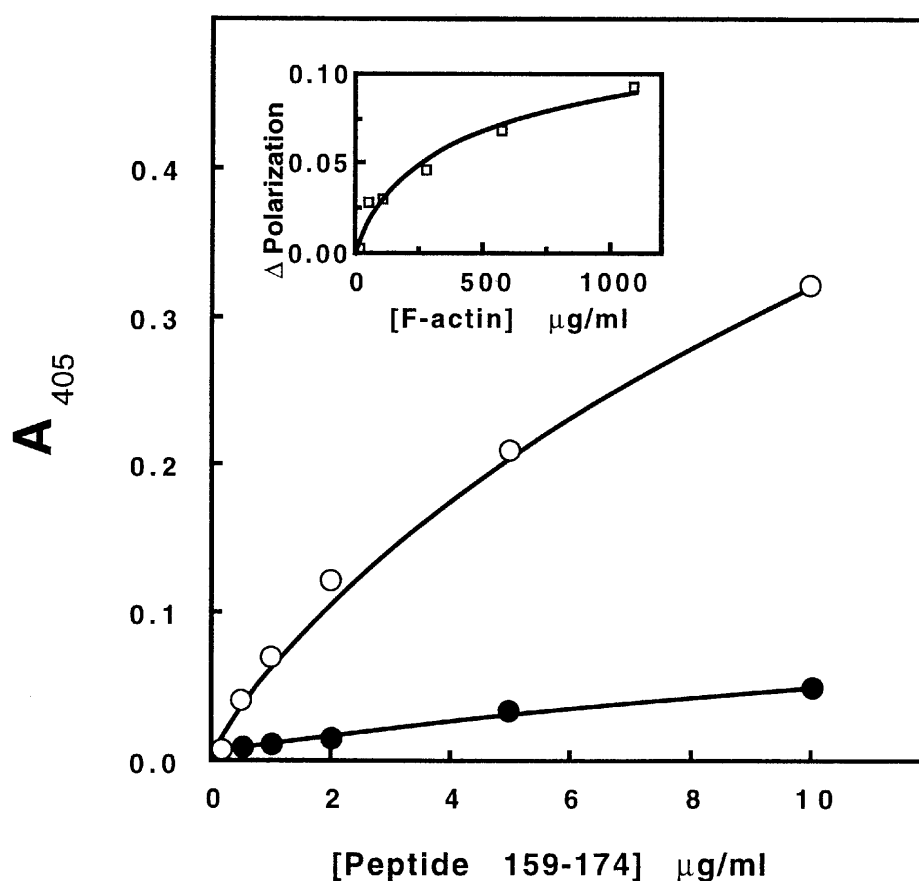


Figure 2 Interaction of actin with the synthetic peptide 159–174. Binding of the peptide (0–10 $\mu\text{g}/\text{ml}$) to coated F-actin ○ was monitored by ELISA. An experiment with coated creatine kinase ● was performed as a control of specificity. The interaction was monitored at 405 nm. Inset: binding of the peptide to F-actin was monitored in solution by using fluorescence polarization. The peptide labelled with NbdCl (20 $\mu\text{g}/\text{ml}$) was incubated with increasing concentrations of F-actin (0–1 mg/ml) and the variation in fluorescence polarization plotted versus F-actin concentration.

Structural Properties of the Synthetic Peptide

The N-terminal sequence of domain 2 including the synthetic peptide (sequence 159–174) belongs to one of the conserved regions in gelsolin and presents sequence similarities with related proteins such as villin [29]. The PHD (Profile Network Prediction Heidelberg) method developed by Rost and Sander [30–32] was applied to this gelsolin region (sequence 154–179), giving the data reported in Figure 1. These suggest that the sequence adopts both extended and loop conformations. A three-dimensional model can also be generated using the Swiss-model computation service (see Material and Methods). The calculation is based on the sequential similarities between subdomain 2 of gelsolin and that of severin, the structure of which has been determined by NMR [22]. The proposed model (Figure 3) shows the presence in this region of two antiparallel extended sequences connected through a loop and stabilized by hydrogen bonds.

Finally, the conformation of the synthetic peptide was checked in aqueous solution (10 mM phosphate, pH 7.5). The secondary structure was studied by Fourier transform IR. Spectral bands in the amide I region associated with definite structures were resolved by spectral deconvolution. The IR spectrum

of the peptide is characterized by the presence of two major bands at 1628 and 1662 cm^{-1} (Figure 4(A)). While the 1628 cm^{-1} associated with the 1685 cm^{-1} band suggests the presence of an antiparallel beta sheet structure, the origin of the 1662 cm^{-1} band is less clear [33]. The presence of a turn conformation, however, cannot be ruled out. The CD spectrum (Figure 4(B)) with a single positive band at 204 nm does not correspond to any well-defined conformation, but could account for the presence of a loop structure [34]

Enhancement of Actin Polymerization by Peptide 159–174

The time course for actin polymerization (in 2 mM Tris, 0.2 mM CaCl_2 , 0.1 mM ATP buffer, pH 7.5) induced by 2 mM MgCl_2 and 0.1 M KCl was studied in the presence of various concentrations of peptide 159–174. F-actin formation was monitored from the fluorescence changes in the pyrenyl fluorophore coupled to actin. As shown in Figure 5(A), the polymerization rate was enhanced in the presence of the peptide, although the extent of polymerization, measured at the end point of the reaction (after at least 24 h) was not greatly altered. Experiments

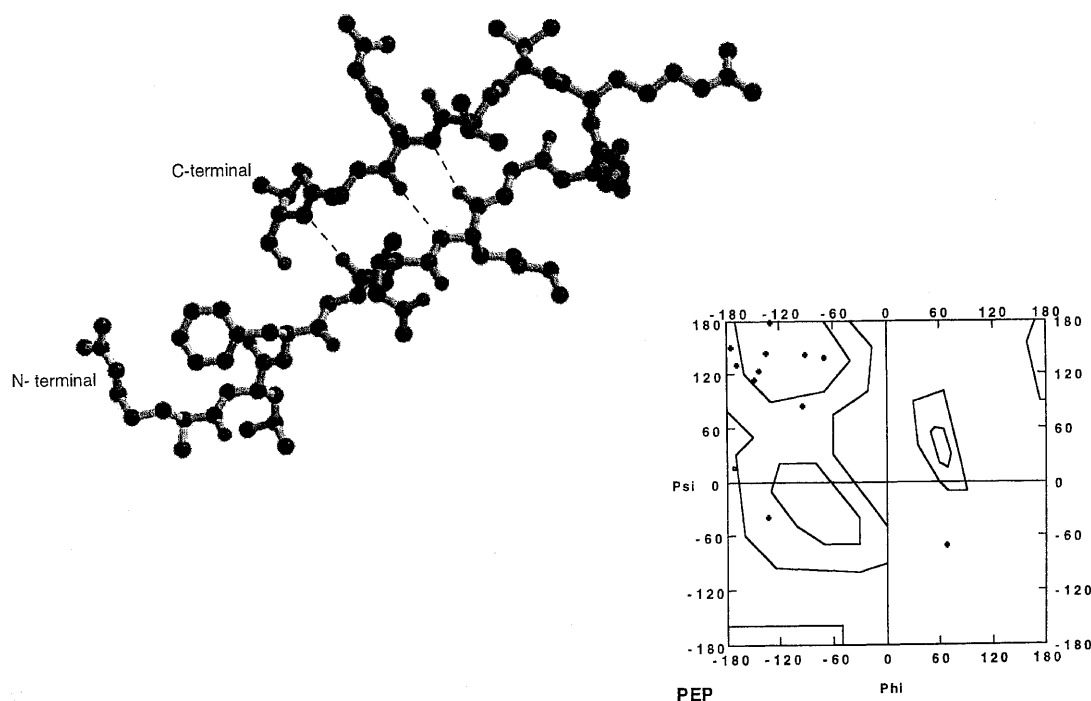


Figure 3 Conformation model of the sequence 161–174. Building of the model was performed using the Swiss-model automatic protein modelling server (see Material and Methods). The potential hydrogen bonds are indicated by broken lines. Inset: Ramachandran plot.

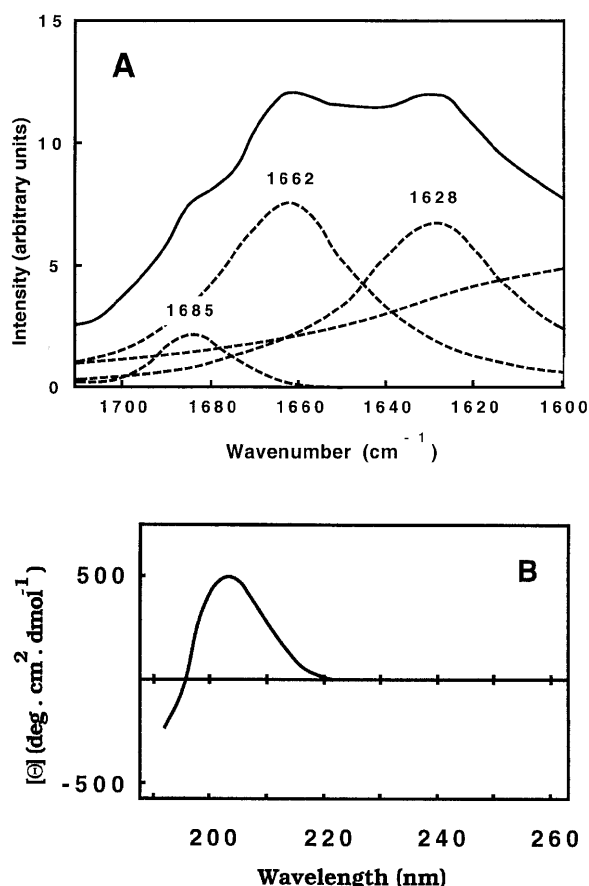


Figure 4 Structure of the synthetic peptide 159–174. (A) IR Fourier transform spectrum. Amide I region of the IR spectrum was observed in 10 mM phosphate, pH 7.5 (—). The corresponding deconvoluted spectra are indicated by broken lines. (B) CD spectrum of the synthetic peptide was observed between 190 and 250 nm in 10 mM phosphate buffer, pH 7.5.

using different concentrations of actin showed only slightly enhanced fluorescence (less than 20%) (Figure 5(B))

Thus, the increased polymerization rate could be related to different changes such as in the elongation rate and/or in the first kinetic steps (nucleus formation and cation exchange kinetics). To distinguish between these possibilities, polymerization from preformed actin nuclei was studied. G-actin was incubated with a small amount of gelsolin (gelsolin : actin molar ratio 1/20) and polymerization induced by salts. As shown in Figure 6, the presence of the peptide did not modify the time course for polymerization. The effect of the peptide on preformed actin filaments was also investigated. Only a very slight modification to the initial rate of actin depolymerization was observed when the peptide

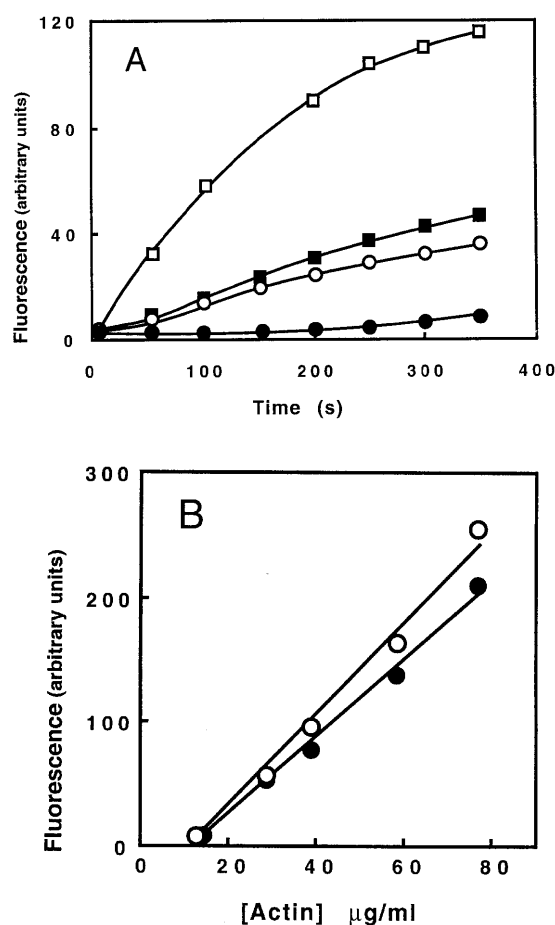


Figure 5 Synthetic peptide-induced enhancement of pyrenyl-actin polymerization by salts, followed by fluorometry. (A) Effect of the peptide on the early steps of actin polymerization. Actin polymerization (400 $\mu\text{g}/\text{ml}$) alone ● or in the presence of the synthetic peptide at 10 $\mu\text{g}/\text{ml}$ ○, 16 $\mu\text{g}/\text{ml}$ ■ and 40 $\mu\text{g}/\text{ml}$ □ was monitored versus time. (B) Effect of the peptide on the end point of actin polymerization. Actin alone ●, actin + peptide at 16 $\mu\text{g}/\text{ml}$ ○.

was present (under 15% at high peptide concentrations, i.e. above 50 $\mu\text{g}/\text{ml}$; Figure 6). These results demonstrate that the effect on polymerization observed in the presence of the peptide can essentially be attributed to an increase in the nucleus formation rate.

A correlation between modifications in the actin polymerization kinetics and possible conformational changes induced by synthetic peptide 159–174 was also considered. The effect of the peptide 159–174 added at various concentrations (in the range reported in Figure 5(A)) on the fluorescence properties of an extrinsic chromophore (AEDANS) linked to actin cys 374 was therefore studied. As shown in Table 1, which reports a typical experiment, an

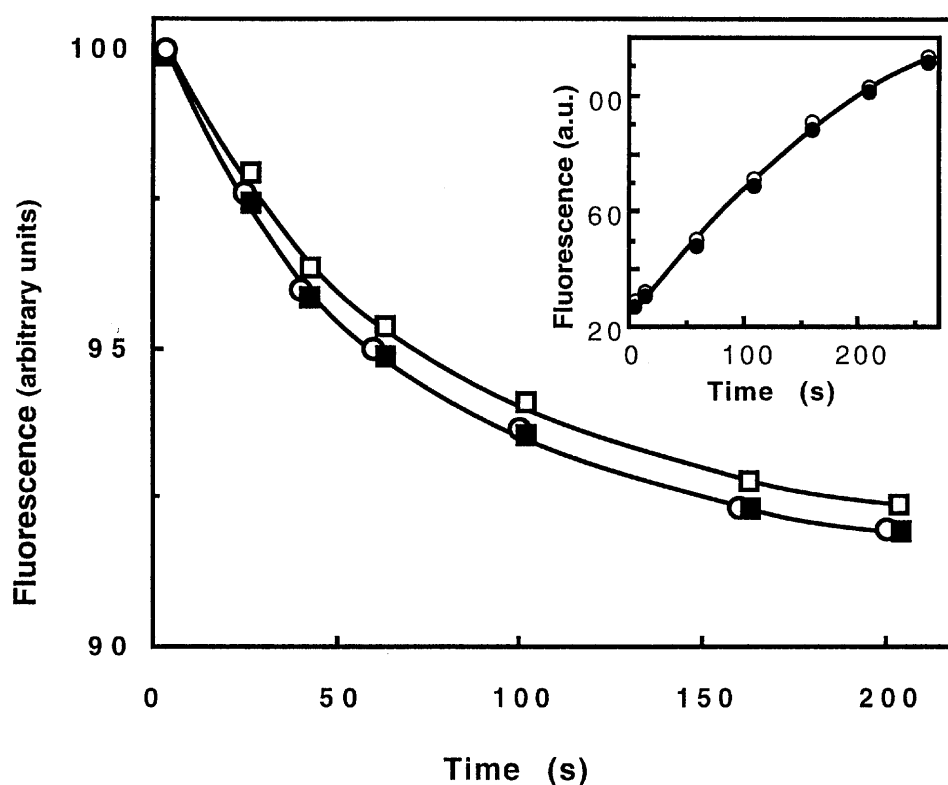


Figure 6 Effect of peptide 159–174 on actin association kinetics. The effect of the peptide on actin filament depolymerization. The fluorescence of pyrenyl-actin is plotted versus time. Actin filaments were diluted to 25 $\mu\text{g/ml}$ at time 0 in the presence of the peptide at 0 \circ , 20 \blacksquare and 50 $\mu\text{g/ml}$ \square . Inset, effect of the peptide on the elongation step. Progress curves show pyrenyl-actin (400 $\mu\text{g/ml}$) polymerization induced by 2 mM MgCl_2 and 0.1 M KCl in the presence of both gelsolin (20 $\mu\text{g/ml}$) and the peptide at 0 \circ and 40 $\mu\text{g/ml}$.

increase in dansyl fluorescence coupled to a slight red shift was observed upon peptide binding. Similar results were obtained with both G- and F-actins. Furthermore, a decrease in the fluorescence of buried tryptophans located in subdomain 1 of unlabelled actin was also observed. These spectral perturbations can be ascribed to environmental modifications around the chromophores, arising from probable changes of actin conformation.

Further studies indicate a significant rise of dansylated actin fluorescence polarization upon

addition of the peptide (Table 1). This can be explained by changes in the dansyl environment induced by peptide binding and/or by an increase in molecular weight linked to the formation of actin oligomers. The latter interpretation was corroborated by two additional direct approaches.

Firstly, the peptide increased the viscosity of a G-actin solution, which was measured with an Oswald microviscosimeter. Specific viscosities were 0.07 ± 0.02 for G-actin (1 mg/ml), 0.23 ± 0.02 for G-actin (1 mg/ml) + peptide 159–174 (40 $\mu\text{g/ml}$) and

Table 1

	Dansylated actin			Intrinsic actin tryptophans	
	Fluorescence (arbitrary units)	Wavelength max. (nm)	Fluorescence polarization	Fluorescence (arbitrary units)	Wavelength max. (nm)
G-actin (60 $\mu\text{g/ml}$)	203	471	0.150	156	333
G-actin (60 $\mu\text{g/ml}$ + peptide (43 $\mu\text{g/ml}$))	245	466	0.170	125	332

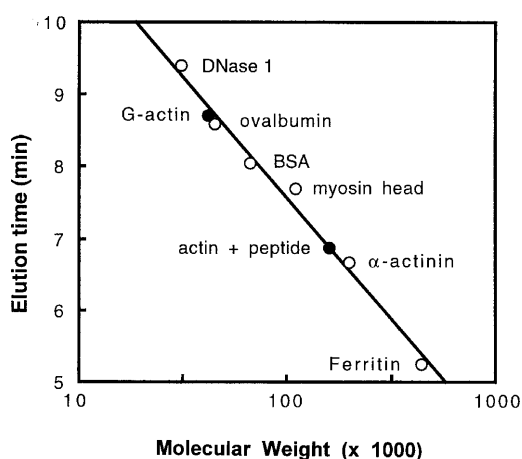


Figure 7 Molecular sieving of actin and actin complexed to peptide 159–174 on a TSK 250 column. Elution time is plotted versus logarithm of molecular weight.

1.22 ± 0.03 for F-actin (1 mg/ml) respectively. Such a viscosity change in the presence of the peptide could result from a major change in the shape of the molecule, but in the case of actin, which has a stable compact structure, the effect observed should rather be attributed to oligomer formation. A similar effect was indeed reported by Magri *et al.* [35] in the case of protamine interaction.

Secondly, in addition to G-actin, some material (about 9%) with a higher apparent Stokes radius than G-actin was detected when the actin–peptide complex was sieved on a TSK column (Figure 7). The peptide can thus induce the formation, in equilibrium with monomeric actin and at low ionic strength (2 mM Tris, 0.2 mM CaCl_2 , 0.1 mM ATP buffer, pH 7.5), of measurable amounts of actin oligomers.

Associated Effect of Peptide and Gelsolin Domain 1 on Actin Polymerization

Several functional assays were conducted to test the effects of peptide 159–174 and of gelsolin domain 1, which binds specifically with the barbed end of actin [12], on actin polymerization kinetics.

As demonstrated below, the polymerization rate of actin was increased by the 159–174 peptide (Figure 5(A)). Moreover, when a low domain 1 concentration (0.8 $\mu\text{g}/\text{ml}$, i.e. 50 nM) to peptide 159–174 (16 $\mu\text{g}/\text{ml}$) for actin polymerization measurements, the initial lag disappeared and there was a dramatic enhancement of the initial polymerization rate compared with the results obtained with the peptide alone (Figure 8(A)). This result is

consistent with an increased nucleation rate, as observed with many capping proteins [2]. The effect on actin filaments was then studied with a depolymerization assay, to determine whether peptide 159–174 with added domain 1 caps F-actin. Actin filaments were diluted in the presence of peptide 159–174 and domain 1 and the beginning of the depolymerization process monitored versus time (Figure 8(B)). The depolymerization rate was considerably reduced in the presence of peptide 159–174 and domain 1 at low concentrations (0.8–1.6 $\mu\text{g}/\text{ml}$, i.e. 50–100 nM). The effect of capZ (added at 2.7 $\mu\text{g}/\text{ml}$, i.e. 40 nM), a well-known capping protein, is also shown for comparison (Figure 8(B)). An estimation of the capping constant was not attempted because the effect depends on the concentrations of the two coupled factors, which apparently act in conjunction with one another.

In another experiment, actin was polymerized overnight in the presence or absence of effectors, and the new equilibrium estimated from the level of pyrenyl fluorescence. As shown in Figure 8(C), fluorescence in the presence of peptide 159–174 and gelsolin domain 1 is slightly lower than in the presence of the peptide alone. The results obtained with non-saturating concentrations of the two ligands and in the presence of various actin concentrations (Figure 8(C)) can be explained by an increase in the apparent critical concentration up to about 0.5 μM . This value is slightly lower than the critical concentration for the pointed end (0.6–0.7 μM) [36] which suggests a capping at the filament barbed end. Two control experiments were also performed. Domain 1 used alone at 50 nM does not significantly modify the equilibrium (not shown). In contrast, as reported below, peptide 159–174 changes the environment of the chromophore linked to actin Cys 374 in actin and slightly enhances the fluorescence of actin without modifying the apparent critical concentration (Figure 5). Therefore, higher nucleation rates, an increased critical concentration and lower depolymerization rates can be explained by a barbed capping process similar to that described for capping proteins such as capZ [2, 37]. Peptide 159–174 derived from gelsolin domain 2 would in fact enhance the intrinsic capping property supported by gelsolin domain 1 [11,12].

DISCUSSION

The binding of gelsolin to the end of the actin filament, and therefore its capping effect, can be in

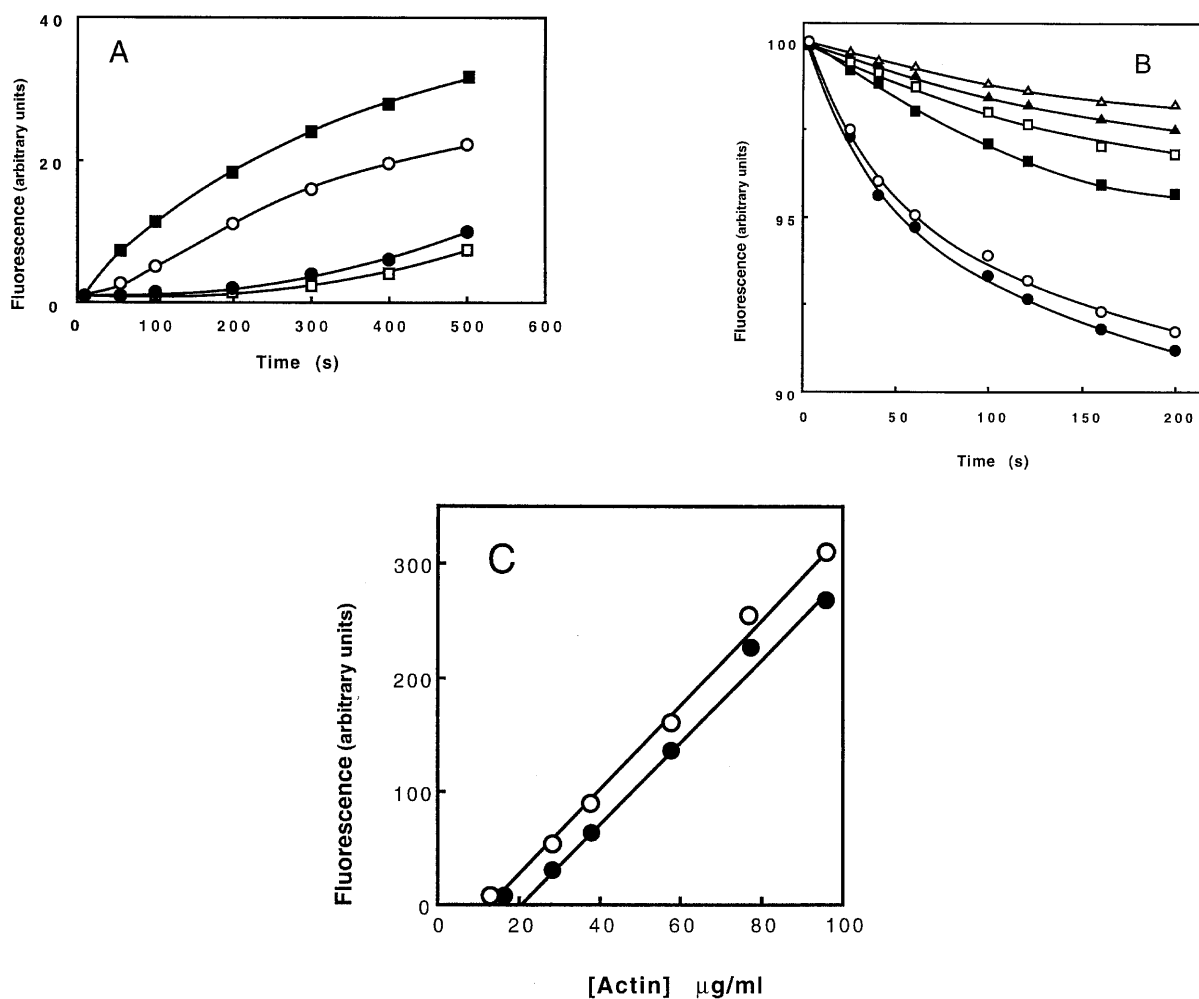


Figure 8 Combined effect of the synthetic peptide 159-174 and purified gelsolin domain 1 on actin polymerization process. (A) Time course of actin polymerization. Actin (200 $\mu\text{g}/\text{ml}$) alone ● or incubated with either domain 1 (0.8 $\mu\text{g}/\text{ml}$) □, or the synthetic peptide (16 $\mu\text{g}/\text{ml}$) ○ or the two peptides at 0.8 $\mu\text{g}/\text{ml}$ and 16 $\mu\text{g}/\text{ml}$ respectively ■. (B) Effect on actin filament depolymerization. The fluorescence of pyrenyl-actin is plotted versus time. Actin filaments were diluted to 25 $\mu\text{g}/\text{ml}$ and the decrease in fluorescence monitored in the absence of effectors ○, in the presence of domain 1 (0.8 $\mu\text{g}/\text{ml}$) ● or domain 1 and peptide 159-174 at 0.8 $\mu\text{g}/\text{ml}$ and 16 $\mu\text{g}/\text{ml}$ ■, at 1.6 $\mu\text{g}/\text{ml}$ and 16 $\mu\text{g}/\text{ml}$ (□ and at 2.0 $\mu\text{g}/\text{ml}$ and 24 $\mu\text{g}/\text{ml}$ △ respectively. Effect of capZ (2.7 $\mu\text{g}/\text{ml}$) was reported as a control ▲. (C) Effect of domain 1 in the presence of the synthetic peptide on the end point of actin polymerization. Fluorescence of actin in the presence of the peptide (16 $\mu\text{g}/\text{ml}$) ○ or the peptide (16 $\mu\text{g}/\text{ml}$) + domain 1 (0.8 $\mu\text{g}/\text{ml}$) ● is plotted versus actin concentration.

part explained by the interaction of domain 1 with the barbed actin end [38]. The interface is located in a cleft between actin subdomains 1 and 3 and includes the apolar exposed face of helix 341-349 [15]. Several authors [12, 38] have demonstrated that gelsolin domain 1 alone, purified either after proteolytic cleavage of the native protein or as a recombinant domain, not only sequesters actin monomers but also binds preferentially to the end

of actin filaments. In addition, segment 1-3, corresponding to the N-terminal half of the gelsolin molecule, severs actin filaments [10, 13, 16], which suggests some cooperation between domains. Subsequently, segment 1-3 efficiently caps actin [10] and impedes any possible reassociation between filaments. An actin site in domain 2 was previously postulated from deletion mutagenesis experiments [12]. It was located between residues 159-173 and

overlapped the phosphoinositide phosphate site [28]. Residues 150–169 in fact constitute a flexible link between the two structured gelsolin domains 1 and 2 [39]. The corresponding synthetic peptide and the same sequence in the entire molecule do not possess a structured conformation [28]. In the presence of TFE, or of some detergents and phosphoinositides, as demonstrated by Xian *et al.* [28], peptide 150–169 is folded into an amphiphilic helical structure including residues 156–166, and a beta sheet conformation towards the C-terminus. A coil-helix transition therefore seems to impede interaction between the actin filament and the gelsolin sites located in domains 1 and 2–3.

The peptide studied here (sequence 159–174) adopts a definite conformation in solution. IR measurements can account for antiparallel beta structure and for the possible presence of a loop. The experimental results are in accordance with both the predictive methods and the putative model, which described the conformation as two antiparallel strands linked by a turn, including residues Arg-168, Arg-169 and Val-170. Model building of a larger part of subdomain 2 including residues 161–233 (not shown) and examination of the homologous structural region of the severin molecule, whose conformation is known from NMR [22], show that peptide 159–174 is a part of the core of gelsolin domain 2 which is composed of five strands surrounded by an alpha helix in the C-terminal.

Peptide 159–174 binds to actin with relatively high affinity although slightly lower than this reported for the whole S2 domain [8]. As gelsolin domains 1 and 2 have some common folding features [15, 22], similar secondary structures might possibly be involved in the binding regions. One major interface in the N-terminal of domain 1 consists of a loop containing Phe-49 and Asp-50 [15]. The interaction of the synthetic peptide would likewise include the turn containing residues Arg-168, Arg-169 and Val-170 and its binding could induce conformational changes in the actin molecule. These structural changes affected at least the environment of Cys-374 and of the two buried tryptophans located in actin subdomain 1 [40]. A change in the orientation of the Cys-374 upon gelsolin binding has been, indeed, recently reported [41]. Using three independent physicochemical approaches, i.e. fluorescence polarization, viscosity and molecular sieving, we also observed that peptide 159–174 at low ionic strength (in the presence of 0.1 mM Ca^{2+}) induced the formation of actin oligomers. A comparable effect has been also reported [7]

for the binding of subfragments 2–3 to G-actin although larger polymers, possibly filaments, were produced.

Another important result is the enhancement of the actin polymerization rate in the presence of the peptide (Figure 5(A)), which can essentially be explained by an increased nucleus formation, without any change in the apparent critical concentration. The peptide would thus induce conformational changes in actin molecule promoting oligomerization. The effect on actin polymerization appears specific as by the low effector concentration needed (μM range). In addition, other polycations were also able to enhance polymerization. Their efficiencies depend mainly upon their structures. So, a short polylysine (M_r 3000) is far less effective than long chains (e.g. 87,000) [42]. In contrast, a heptapeptide derived from cofilin (used in the millimolar range) promotes actin nuclei formation, its efficiency being dependent upon heptapeptide sequence [43].

The domain 2 from which the peptide 159–174 is derived, in association with domain 1, apparently also plays an active role in gelsolin capping [13]. The combination of domain 1 and peptide 159–174 dramatically modifies the actin polymerization properties.

Firstly, nucleation experiments show that peptide 159–174 in the presence of gelsolin domain 1 accelerates the nucleation process more markedly than does the peptide alone. This property is specific to the synthetic peptide, since domain 1 does not increase nucleation at all [38]. The nucleating activity of segment 1–3 is subject to contradictory reports. Bryan and Hao [44] and Chaponnier *et al.* [45] reported that the amino-terminal half-fragment obtained by gelsolin proteolysis promotes nucleation but that the effect is less than with whole gelsolin. In contrast, Way *et al.* [10], using a recombinant fragment, did not observe any nucleating activity at all. A further result [10] suggests, however, that domain 2 promotes nucleation. Domains 2–6 show evidence of nucleating activity while domains 4–6 alone do not.

Secondly, domain 1 is known to interact with the barbed end of the actin filament [15] and it was found that when added to peptide 159–174 it decreased the pyrenyl fluorescence of actin polymerized to steady state. This was consistent with high affinity capping at the barbed end. We observed an increase in the apparent critical concentration, which can be accounted for by the higher critical concentration known to be present at the pointed end compared with the barbed end.

Thirdly, the pyrenyl-actin depolymerization assay showed a greatly reduced depolymerization rate when the two fragments were used together at low concentrations. Inhibition was dependent on the concentrations of each component. Depolymerization experiments indicated that capping efficiency is similar to that observed with capZ protein. Neither domain 1 nor domains 2–3 cap as well as whole gelsolin [12]. Nevertheless, the cooperative effect of domain 1 and a peptide derived from domain 2 can provide efficient capping.

In conclusion, this study provides some insight into the dynamic process needed for capping activities of gelsolin. In particular, we show that small synthetic peptides can be folded into an active structure. Our experimental data are consistent with the notion that both the synthetic peptide 159–174 and domain 2 of gelsolin can induce changes in actin conformation and in the kinetics of actin polymerization. The participation of other actin sites in domain 2, its link with domain 1 and the conformational effect of domain 3 appear to be important parameters determining the properties of the gelsolin N-terminal half.

Acknowledgements

This research was supported by grants from the 'Association Française contre les Myopathies' and the IFREMER.

REFERENCES

1. V. T. Nachmias, R. Golla, J. F. Casella and E. Barron-Casella (1996). Cap Z, a calcium insensitive capping protein in resting and activated platelets. *FEBS Lett.* **387**, 258–262.
2. J. A. Cooper and T. D. Pollard (1985). Effect of capping protein on the kinetics of actin polymerization. *Biochemistry* **24**, 793–799.
3. B. Pope, M. Way and A. G. Weeds (1991). Two of the three actin-binding domains of gelsolin bind to the same subdomain of actin. Implications of capping and severing mechanisms. *FEBS Lett.* **280**, 70–74.
4. T. P. Stossel (1993). On the crawling of animal cells. *Science* **260**, 1086–1094.
5. C. C. Cunningham, T. P. Stossel and D. J. Kwiatkowski (1991). Enhanced motility in NIH 3T3 fibroblasts that overexpress gelsolin. *Science* **251**, 1233–1236.
6. R. G. Watts (1995). Role of gelsolin in the formation and organization of triton soluble F-actin, during myeloid differentiation of HL-60 cells. *Blood* **85**, 2212–2221.
7. J. Bryan, (1988). Gelsolin has three actin-binding sites. *J. Cell. Biol.* **106**, 1553–1562.
8. M. Way, B. Pope and A. G. Weeds (1992). Evidence for functional homology in the F-actin binding domains of gelsolin and alpha-actinin: Implications for the requirements of severing and capping. *J. Cell. Biol.* **119**, 835–842.
9. T. Hellweg, H. Huissen and W. Eimer (1993). The Ca(2+)-induced conformational change of gelsolin is located in the carboxyl-terminal of the molecule. *Biophys. J.* **65**, 799–805.
10. M. Way, J. Gooch, B. Pope and A. G. Weeds (1989). Expression of human plasma gelsolin in *Escherichia coli* and dissection of actin binding sites by segmental deletion mutagenesis. *J. Cell Biol.* **109**, 593–605.
11. M. Way, B. Pope and A. G. Weeds (1992). Are the conserved sequences in segment 1 of gelsolin important for binding actin? *J. Cell Biol.* **116**, 1135–1143.
12. H. Q. Sun, D. C. Wooten, P. A. Janmey and H. L. Yin (1994). The actin side-binding domain of gelsolin also caps actin filaments. Implication for actin filament severing. *J. Biol. Chem.* **269**, 9473–9479.
13. M. Way and P. Matsudaira (1993). The secrets of severing? *Current Biol* **3**, 887–890.
14. J. Feinberg, Y. Benyamin and C. Roustan (1995). Definition of an interface implicated in gelsolin binding to the sides of actin filaments. *Biochem. Biophys. Res. Commun* **209**, 426–432.
15. P. J. McLaughlin, J. T. Gooch, H. G. Mannhertz and A. G. Weeds (1993). Structure of gelsolin segment 1-actin complex and the mechanism of filament severing. *Nature* **364**, 685–692.
16. A. McGooch and M. Way (1995). Molecular model of an actin filament capped by a severing protein. *J. Struct. Biol.* **115**, 144–150.
17. J. A. Spudich and S. Watt (1971). The regulation of rabbit skeletal muscle contraction. I. Biochemical studies of the interaction of the tropomyosin-troponin complex with actin and the proteolytic fragments of myosin. *J. Biol. Chem.* **249**, 4866–4871.
18. R. Takashi (1979). Fluorescence energy transfer between subfragment-1 and actin points in the rigor complex of actosubfragment-1. *Biochemistry* **18**, 5164–5169.
19. T. Kouyama and K. Mihashi (1981). Fluorometry study of N-(1-pyrenyl)iodoacetamide-labelled F-actin. Local structural change of actin protomer both on polymerization and on binding of heavy meromyosin. *Eur. J. Biochem.* **114**, 33–38.
20. Z. Soua, F. Porte, M. C. Harricane, J. Feinberg and J. P. Capony (1985). Bovin serum brevin. Purification by hydrophobic chromatography and properties. *Eur. J. Biochem.* **153**, 275–287.
21. J. Feinberg, J. P. Capony, Y. Benyamin and C. Roustan (1993). Definition of the EGTA-independent interface involved in the serum gelsolin-actin complex. *Biochem. J.* **293**, 813–817.

22. A. Schunckel, R. Wiltschek, L. Eichinger, M. Schleicher and T. A. Holak (1995). Structure of severin domain 2 in solution. *J. Mol. Biol.* **247**, 21–27.
23. M. C. Peitsch (1996). Promod and Swiss-model: Internet-based tools for automated comparative protein modelling. *Biochem. Soc. Trans.* **24**, 274–279.
24. B. R. Brooks, R. E. Bruceoleri, B. D. Olafson, D. J. Stats, S. Swaminathan and M. Karplus (1983). A program for macromolecular energy minimization and dynamic calculations. *J. Comp. Chem.* **4**, 187–217.
25. J.P. Labbé, M. Boyer, C. Roustan and Y. Benyamin (1992). Localization of a myosin subfragment 1 interaction site on the C-terminal part of actin. *Biochem. J.* **284**, 75–79.
26. C. Mejean, M. C. Lebart, M. Boyer, C. Roustan and Y. Benyamin, (1992). Localization and identification of actin structures involved in the filamin-actin interaction. *Eur. J. Biochem.* **209**, 555–562.
27. C. Frieden (1983). Polymerization of actin mechanism of the Mg^{2+} induced proceed at pH 8 and 20°C. *Proc. Natl. Acad. Sci. USA* **80**, 6513–6517.
28. W. Xian, R. Vegners, P. A. Janmey and W. H. Braunlin (1995). Spectroscopic studies of a phosphoinositide-binding peptide from gelsolin: Behaviour in solutions of mixed solvent and anionic micelles. *Biophys. J.* **69**, 2696–2702.
29. M. Arpin, E. Pringault, J. Finidori, A. Garcia, J. M. Jeltsch, J. Vandekerckhove and D. Louvard (1988). Sequence of human villin: A large duplicated domain homologous with other actin-severing proteins and a unique small carboxyl-terminal related to villin specificity. *J. Cell Biol.* **107**, 1759–1766.
30. B. Rost (1996). PHD: Predicting one-dimensional protein structure. *Methods. Enzymol.* **266**, 525–539.
31. B. Rost and C. Sander (1993). Prediction of protein secondary structure at better than 70% accuracy. *J. Mol. Biol.* **232**, 584–599.
32. B. Rost and C. Sander (1994). Combining evolutionary information and neural networks to predict protein secondary structure. *Proteins* **19**, 55–72.
33. A. Dong, P. Huang and W. S. Caughey (1990). Protein secondary structures in water from second-derivative amide I infrared spectra. *Biochemistry* **29**, 3303–3308.
34. L. M. Gierasch, C. M. Deber, V. Madison, C. H. Niu and E. R. Blout (1981). Conformations of (X-L-Pro-Y)₂ cyclic hexapeptides. Preferred beta-turn conformers and implications for beta-turns in proteins. *Biochemistry* **20**, 4730–4738.
35. E. Magri, M. Zaccarini and E. Grazi (1978). Does protamine dictate the direction of growth of the actin filaments? *Biochem. Biophys. Res. Commun.* **85**, 35–41.
36. C. Hug, T. M. Miller, M. A. Torres, J. F. Casella and J. A. Cooper (1992). Identification and characterization of an actin-binding site of CapZ. *J. Cell Biol.* **116**, 923–931.
37. S. E. Caldwell, S. G. Heiss, V. Mermall and J. A. Cooper (1989). Effect of CapZ, an actin capping protein of muscle, on the polymerization of actin. *Biochemistry* **28**, 8506–8514.
38. A. Weber, M. Pring, S. L. Lin and J. Bryan (1991). Role of the N- and C-terminal actin-binding domains of gelsolin in barbed filament end capping. *Biochemistry* **30**, 9327–9334.
39. D. J. Kwiatkowski, T. P. Stossel, S. H. Orkin, J. E. Mole, H. R. Colten and H. L. Yin (1986). Plasma and cytoplasmic gelsolins are encoded by a single gene and contain a duplicated actin-binding domain. *Nature* **323**, 455–458.
40. I. Kuznetsova, O. Antropovax, K. Turoverov and S. Khaitlina (1996). Conformational changes in subdomain 1 of actin induced by proteolytic cleavage within the DNase I-binding loop: Energy transfer from tryptophan to AEDANS. *FEBS Lett.* **383**, 105–108.
41. E. Prochniewicz, Q. Zhang, P. A. Janmey and D. D. Thomas (1996). Cooperativity in F-actin: Binding of gelsolin at the barbed end effects structure and dynamics of the whole filament. *J. Mol. Biol.* **260**, 756–766.
42. D. C. Lin, K. D. Tobin, M. Grumet and S. Lin (1980). Cytochalasins inhibit nuclei-induced actin polymerization by blocking filament elongation. *J. Cell Biol.* **84**, 455–460.
43. N. Yonezawa, E. Nishida, M. Obha, M. Seki, H. Kumagai and H. Sakai (1989). An actin-interacting hexapeptide in the cofilin sequence. *Eur. J. Biochem.* **183**, 235–238.
44. J. Bryan and S. Hwo (1986). Definition of an N-terminal actin-binding domain and a C-terminal Ca^{2+} regulatory domain in human brevin. *J. Cell Biol.* **102**, 1439–1446.
45. C. Chaponnier, P. A. Janmey and H. L. Yin (1986). The actin filament-severing domain of plasma gelsolin. *J. Cell Biol.* **103**, 1473–1481.